Modeling Earth Systems and Environment
https://doi.org/10.1007/s40808-022-01389-4

ORIGINAL ARTICLE

Earlier green-up and senescence of temperate United States rangelands under future climate

Scott N. Zimmer[1,2] · Matthew C. Reeves[3] · Joseph R. St. Peter[4] · Brice B. Hanberry[5]

Received: 20 December 2021 / Accepted: 1 April 2022

Abstract
Climate and vegetation phenology are closely linked, and climate change is already impacting phenology in many systems. These impacts are expected to progress in the future. We sought to forecast future shifts in rangeland growing season timing due to climate change, and interpret their importance for land management and ecosystem function. We trained a model on remotely sensed land surface phenology and climate data collected from 2001 to 2014 in temperate United States rangelands. We used this model to forecast annual growing season start dates, end dates, and season length through 2099 among six general circulation models and under RCP 4.5 and 8.5 scenarios. Growing season start was projected to shift earlier throughout our study area. In 2090–2099, start of season advanced by an average of 10 (RCP 4.5) to 17 (RCP 8.5) days. End of season also advanced by 12 (RCP 4.5) to 24 (RCP 8.5) days, but with greater heterogeneity. Start and end of season change mainly offset one another, so growing season length changes were lesser (2 days in RCP 4.5, and 7 in RCP 8.5). Some mountainous areas experienced both earlier start of season and later end of season, lengthening their growing season. Earlier phenology in rangelands would force adaptation in grazing and impact ecosystem function. Mountainous areas with earlier start and later end of season may become more viable for grazing, but most areas may experience slightly shortened growing seasons. Autumn phenology warrants greater research, and our finding of earlier autumn senescence contradicts some prior research.

Keywords Climate change · Forecast · Growing season · Model · Phenology · Vegetation dynamics

Introduction

Phenology is the study of periodic events, factors that influence their timing, and relationships among such events (Lieth 1974). Individual species, communities, ecosystem function and services, biogeochemical cycles, vegetation–climate feedbacks, and agriculture all respond to phenological cycles (Richardson et al. 2013; Piao et al. 2019). Vegetation phenology is one such periodic cycle of plant growth and is driven by three basic factors: sunlight, water, and temperature (Zhao et al. 2013).

Field observations of distinct events like vegetation leaf-out or bloom have historically been the basis of vegetation phenology research and still provide important phenological data (Leopold and Jones 1947; Menzel 2002). However, applications to study phenology from remotely sensed imagery have grown rapidly since imagery from sensors such as Landsat-1 and AVHRR became widely available (Henebry and de Beurs 2013), because such satellite imagery can detect broad spectral changes associated with vegetation green-up and senescence (Reed et al. 1994; Stöckli and Vidale 2004). This field became known as "land surface phenology" because these remotely sensed phenological changes represent the aggregate activity of vegetation in a given area, rather than the phenology of individual species (Hanes et al. 2014). Land surface phenology allows research across much broader spatial and temporal scales than traditional in situ

✉ Scott N. Zimmer
scottnzimmer@gmail.com

1 Climate Adaptation Science Program, Utah State University, Logan, UT, USA

2 Uncompahgre Field Office, Bureau of Land Management, Montrose, CO, USA

3 Rocky Mountain Research Station, Human Dimensions Program, USDA Forest Service, Missoula, MT, USA

4 School of the Environment, Center for Spatial Ecology and Restoration, Florida A&M University, Tallahassee, FL, USA

5 Rocky Mountain Research Station, USDA Forest Service, Rapid City, SD, USA

Published online: 27 April 2022

observations and is particularly suited to examining phenological shifts over time and across regions.

Climate and phenology are closely linked, so phenology serves as a biological indicator of climate change (Cleland et al. 2007). Generally, temperature is the primary factor influencing spring vegetation phenology in temperate and mid to high latitude regions where growing seasons are warm and dormant seasons are cold (Walther et al. 2002; Linderholm 2006; Wu and Liu 2013; Fu et al. 2020). Land surface phenology studies strongly indicate an advancement in the timing of spring vegetation green-up globally in the last few decades, widely credited to rising temperatures (Parmesan and Yohe 2003; Linderholm 2006; Julien and Sobrino 2009; Richardson et al. 2013; Piao et al. 2019). This earlier spring timing is also supported by climatic indices of spring onset (Schwartz et al. 2006).

Climate change effects on autumn phenology have largely not received as much attention as effects on spring phenology (Gallinat et al. 2015), but impacts to autumn dynamics may be as significant and more varied (Walther et al. 2002; Richardson et al. 2013; Garonna et al. 2014; Liu at al. 2016). Climatic controls on autumn phenology are less clear than those to spring phenology, with interactions between temperature, moisture, and photoperiod playing roles (Estrella and Menzel 2006; Way and Montgomery 2015; Ren et al. 2018a; Fu et al. 2020). Broad analyses have generally shown that climate change has delayed autumn senescence, which, along with earlier spring green-up, has consequently lengthened growing seasons (Stöckli and Vidale 2004; Linderholm 2006; Julien and Sobrino 2009; Jeong et al. 2011; Ge et al. 2015).

Phenology research has largely focused on forested ecosystems (Richardson et al. 2013), so phenology impacts in grasslands may not exhibit the spring advancement and autumn delay often found in more global analyses. For example, Ying et al. (2020) found autumn senescence delays in Inner Mongolia forest and forest steppe, but advancement in non-forested ecosystems. Similarly, autumn senescence might be occurring later throughout much of the Northern Hemisphere, but earlier in the predominantly non-forested western USA (Piao et al. 2007). Studies specific to grasslands have also supported autumn senescence advancement (Li et al. 2016; Ren et al. 2018b), and warmer temperatures have been shown in experiments to advance grassland autumn senescence (Zavaleta et al. 2003). These studies and others have also found support of spring green-up advancement in grasslands (Piao et al. 2007; Zhang et al. 2013; Li et al. 2016; Chang et al. 2017; Ren et al. 2018b), in line with more global findings. However, some have found delays in grassland spring green-up (Reed 2006; Yu et al. 2010), or advances during some time frames and delays in others (Piao et al. 2011; Wu and Liu 2013).

Though species-specific phenology models at local scales are well advanced, generalized models of phenology at large extents can be improved (Piao et al. 2019). Jolly et al. (2005) developed a generalized growing season phenology model from photoperiod, minimum temperatures, and vapor pressure deficit to address phenological timing at model sites. Xin et al. (2015) expanded this work by modeling growing season start dates in United States (US) grasslands through multiple methods, including variants of the Jolly et al. (2005) growing season index. Their models achieved reasonable accuracy in predicting growing season onset across this large study area. However, they did not model growing season end, and consequently could not address vegetation senescence or growing season length. Hufkens et al. (2016) used PhenoCam imagery to model future dynamics in western USA and Canadian grasslands, and projected earlier spring green-up and later autumn senescence, consequently lengthening growing seasons.

Changes to spring green-up, autumn senescence, and overall growing season length have important implications for grasslands, including impacts on global carbon cycling (Piao et al. 2007; Richardson et al. 2013), wildlife migration (Monteith et al. 2011), and land uses such as grazing (Ren et al. 2018b). Models of future phenological changes, particularly those that address grasslands and autumn senescence, are lacking. Planning of future climate adaptation in these ecosystems could be greatly improved by such projections of future phenological impacts. To address this need, we developed a generalized model of climatic impacts on phenology in temperate US rangelands. We then projected this model through the year 2099 under six general circulation models and RCP 4.5 and 8.5 scenarios to address how future climatic conditions will influence rangeland growing season timing.

Methods

Study area

We limited our study area to locations defined as rangelands by Reeves and Mitchell (2011) within the western USA. We further restricted the study area to a subset of rangelands, as described in Input data. To summarize the results geographically, we evaluated our results throughout major ecological provinces (McNab et al. 2007) in the study area (Fig. 1). This area includes a diversity of shrubland and grassland environments, and much of it is managed by federal agencies such as Bureau of Land Management and US Forest Service.

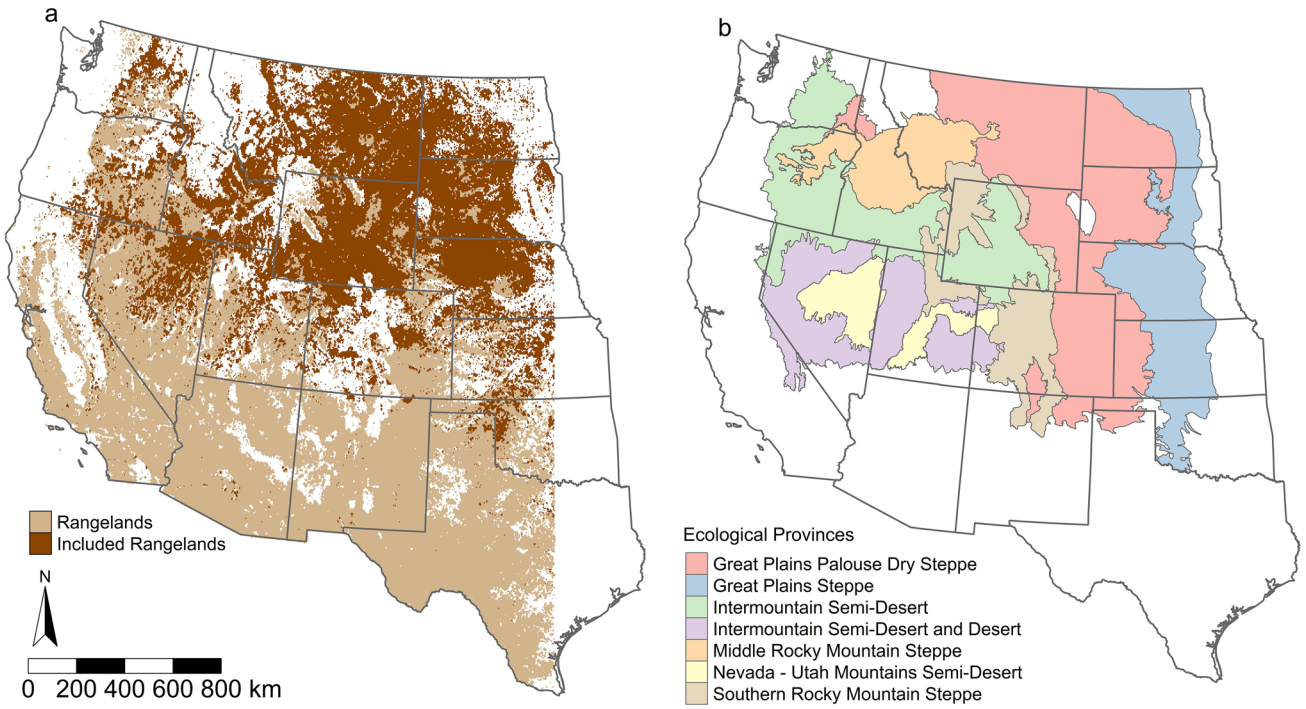

Fig. 1 Maps of the study area showing all rangelands and the subset included in modeling (**a**), and the major ecological provinces encompassing the included rangelands (**b**)

Model overview

We sampled elevation, daily climate, and daily growing season determinations from 2001 to 2014 from more than 2000 random pixels throughout the study area. We utilized these data to train and validate models of annual growing season timing. We modeled start of season (SOS) dates, end of season (EOS) dates, and growing season length (GSL) through a two-step process (Fig. 2). We first employed a binomial generalized linear model to predict the probability that each day in a year fell within the growing season. This model was fit with daily climate and elevation data, and trained on USGS eMODIS growing season determinations.

Next, using the set of daily growing season probabilities in each year, we needed to determine which dates represented growing season start and end. To accomplish this, we fit a sinusoidal model to the growing season probabilities, and determined when the fit line surpassed and fell below given growing season probabilities. Lastly, growing season length was calculated as the difference between the determined EOS and SOS dates. Future projections were made with the same models, using elevation and future projected climate as inputs.

Input data

We used phenology products from USGS eMODIS Collection 5 Terra Western as the measure of growing season timing from 2001 to 2014 in the study area (Jenkerson et al. 2010; Brown 2016; USGS EROS 2018). These phenology data are well-established metrics of growing seasons in the study area, and have been utilized in many studies of phenology (see Howard et al. 2012; Gu et al. 2013; Liebezeit et al. 2014; Boyte et al. 2015; Meier et al. 2015; Zhou et al. 2019). We utilized SOS (start of season time) and EOS (end of season time) data from eMODIS. These metrics are derived by calculating a time series of smoothed NDVI data, calculating a 14-day delayed moving average of NDVI from the smoothed NDVI values, and determining when these lines intersect (Reed et al. 1994; Meier and Brown 2014). These intersections indicate either a sharp increase or decrease in NDVI, signaling either the onset or end of the year's growing season (Meier and Brown 2014). This process reduces sensitivity to temporary NDVI trend changes and measurement errors from factors such as cloud contamination (Reed et al. 1994). However, snowmelt can confound vegetation green up identified by this method, so some have produced

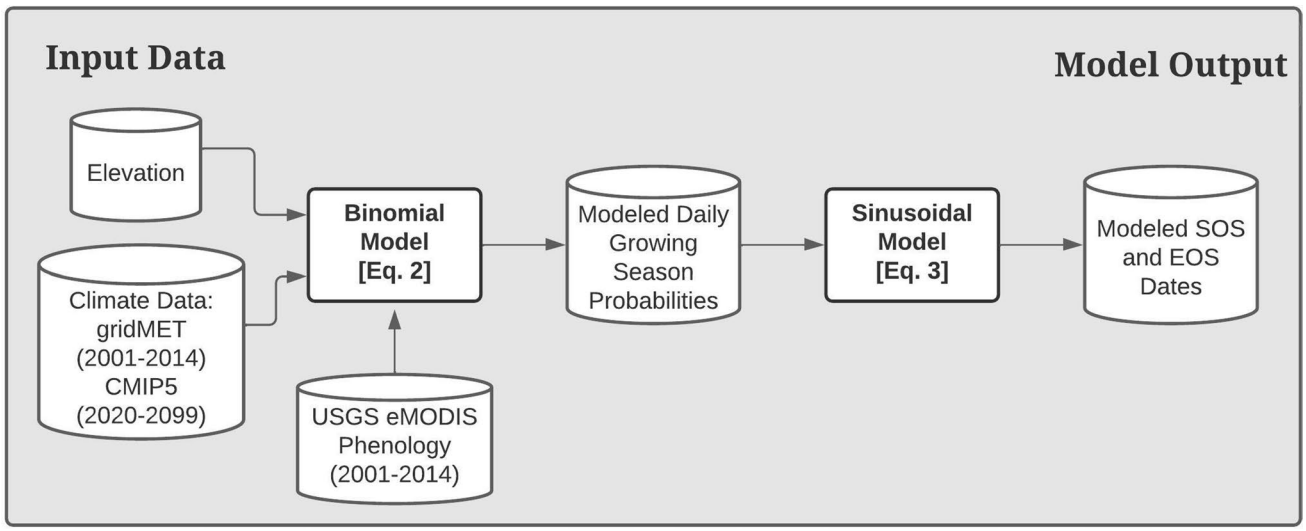

Fig. 2 Flowchart of modeling process. Models were fit with elevation, daily gridMET climate from 2001 to 2014, and USGS eMODIS phenology from 2001 to 2014. Future projections were made using the same models, with elevation and daily CMIP5-projected climate data from 2020 to 2099

alternative phenology indices without the influence of snowmelt (Delbart et al. 2006; Gallant et al. 2018; Wang et al. 2018). These indices may somewhat improve phenology determinations, but are still somewhat novel approaches and may be most necessary in evergreen forests, not grasslands (Beck et al. 2006; Gallant et al. 2018).

From the eMODIS SOS and EOS dates, we produced a binary record of whether dates fell within the year's growing season. For example, if the SOS was day 90 and EOS was day 300 at a given pixel in a given year, days 1–89 were not within the growing season at that pixel in that year, days 90–300 were within the growing season, and days 301–365 were not within the growing season. Dates not within the growing season were coded as 0, and dates within the growing season were coded as 1.

We associated these binary growing season data with gridMET daily climate data at 4 km resolution (Abatzoglou 2013), including maximum temperature, minimum temperature, and downward shortwave radiation. Growing degree days (GDD) were calculated daily from mean daily temperature minus a base temperature of 0ºC, and were cumulatively summed over the year to calculate accumulated growing degree days (AGDD). The base temperature of 0 ºC is commonly used in temperate grasslands (Frank and Hofmann 1989; Preister et al. 2019). While individual species have varying base temperatures, 0 ºC is suitable for temperate grasslands as a whole, and manipulations of base temperature have little effect on GDD correlations to phenology (Romano et al. 2014). Exploratory data analysis showed the AGDD value of 2500 was strongly associated with growing season end throughout our study area, so we calculated whether this threshold had been surpassed and if so by how much, and included this as a variable in modeling. Vapor pressure deficit (VPD) was estimated from the difference between saturated vapor pressure at daily maximum and minimum temperatures by the following equation from Lobell et al. 2014:

$$\mathrm{VPD} = \left(0.6107 * e^{17.269 T_{\max}/(237.3 + T_{\max})}\right) - \left(0.6107 * e^{17.269 T_{\min}/(237.3 + T_{\min})}\right). \quad (1)$$

Phenology in annual grasslands and deserts is highly variable, with the potential for multiple growing seasons annually and start of season occurring as early as autumn in some years (Reed et al. 1994). To assess only locations with a single annual growing season and avoid such highly variable regions, we removed locations with start of season dates earlier than January 1 or later than May 30 in any years (Fig. 1a). This filtering also eliminated areas which may have experienced major vegetation shifts or disturbances during the study period. This was desirable because we were interested only in the effects of climate, not vegetation change, on phenology timing.

Binomial growing season probability model

We used a binomial generalized linear model in R (R Core Team 2018) to fit daily climate and elevation data to daily growing season determinations. We included seven variables in the binomial model (Table 1). This binomial model predicted the probability that a given day fell within the year's growing season for all included pixels.

Table 1 Variables included in the generalized linear model

Variable	Definition
GS	Record of whether day fell within the year's growing season
SRAD	Downward shortwave radiation (W * m^{-2})
VPD	Vapor pressure deficit (Pa)
TMAX	Maximum temperature (C)
AGDD	Accumulated growing degree days in the year to date
AGDD-2500	How far AGDD was above the threshold of 2500, if this threshold had been surpassed
Elev	Elevation (m)

The model was fit with a logit link with the following equation, where variable notations match those in Table 1, β_0 represents the equation's intercept, and β_1 through β_6 represent variable coefficients (shown in Table S1). All climatic variables correspond to measurements from a single day, d, and μ represents the probability that the given day fell within the growing season:

$$\ln\left(\frac{\mu}{1-\mu}\right) = \beta_0 + \beta_1 \mathrm{SRAD}_d * \beta_2 \mathrm{VPD}_d * \beta_3 \mathrm{TMAX}_d * \beta_4 \mathrm{AGDD}_d + \beta_5 \mathrm{Elev} + \beta_6 \mathrm{AGDD} - 2500_d \quad (2)$$

Of the 2000 random pixels from which we sampled climate and growing season data, we randomly selected a small subset (14% of pixels) for training the model. Data from the remaining pixels were reserved for model validation. We further restricted the input data by selecting 9 years of climate and phenology records for training the model, and reserved 5 years for model validation. The training years were manually selected to include years with varying phenological conditions (e.g., years with early, late, and typical growing seasons across the study area), training the model on a wide set of conditions. The years reserved for model validation were: 2003, 2005, 2008, 2012, and 2014.

The model was fit using only the training pixels, with climate and phenology data from only the training years. Model accuracy was evaluated using validation pixels, with climate and phenology data from validation years.

Sinusoidal growing season dates model

The binomial model output daily growing season probabilities for each year. From these daily probabilities, growing season start and end dates had to be determined. To accomplish this, we fit a sinusoidal model to the set of daily growing season probabilities. Phenological data are well fit by sinusoidal models because of their strong periodicity (see Hogg et al. 2000; Girondot et al. 2006). We applied the following second harmonic sinusoidal model (similar to one outlined in Sapiano et al. 2012), where *GS Prob* is growing season probability, d is the day of the year, and w is the cycle's frequency ($2\pi/365$ days). B_0 represents the model intercept, B_1–B_4 represent variable coefficients, and ε represents error:

$$\mathrm{GS\ Prob}(d) = \beta_0 + \beta_1 \sin(d * w) + \beta_2 \cos(d * w) + \beta_3 \sin(d * 2w) + \beta_4 \cos(d * 2w) + \varepsilon. \quad (3)$$

The sinusoidal model was fit at each pixel in each year. The resulting set of fit probabilities from the model was then analyzed to determine the day when the fit probability first surpassed 0.5, and the day when it next fell below 0.45. These dates were interpreted as the start of season date, and the end of season date, respectively, at a given pixel in a single year. Model validation showed these thresholds best aligned with eMODIS SOS and EOS dates throughout the study area.

Though other methods can allow more direct biophysical interpretations of factors beyond growing season start and end (Garroutte et al. 2016; Morisette et al. 2021), these interpretations were not possible in our case because our model fit modeled growing season probability rather than NDVI, EVI, or other direct vegetation indices.

Projecting future growing season dates

We projected future growing season dates by running the binomial growing season probability and sinusoidal growing season dates models with future projected climate. We utilized CMIP5 projections (Taylor et al. 2012) downscaled using the MACA method (Abatzoglou and Brown 2012). The following six global climate models (GCMs) under RCP 4.5 and 8.5 scenarios were resampled to a common 4-km resolution and utilized in modeling: BCC-CSM1.1 (m), CNRM-CM5.1, HadGEM2-ES, IPSL-CM5A-MR, MRI-CGCM3, and NorESM1-M. These models were chosen because they capture a range of possible future climatic conditions and are used in the Forest Service 2020 Resources Planning Act (RPA) Assessment (Joyce and Coulson 2020), which utilizes these projections.

For each GCM/RCP combination, we used the binomial model to predict daily growing season probabilities from 2020 to 2099, then used the sinusoidal model to determine SOS and EOS dates from these probabilities for each pixel and in each year. Growing season length (GSL) was calculated as the difference between EOS and SOS dates. We compared the future projected growing season dates to the mean growing season dates predicted by the model at each pixel during the baseline period (2001–2014) to quantify the projected growing season changes relative to current conditions. We evaluated changes in SOS date, EOS date, and GSL.

We obtained ensemble projections of change for each year by calculating the mean of projected changes from all GCMs

in each year under both RCP scenarios. For example, we calculated the mean of projected changes from the six GCMs under RCP 4.5 in the year 2030 to obtain the ensemble projection of change for this year under RCP 4.5. Lastly, we calculated the mean of ensemble projections across decades (from 2030 to 2039, 2040–2049, etc.) to determine more stable projected changes without annual climatic variability.

Since our model was trained on eMODIS land surface phenology metrics, our results should be interpreted as projected changes in these phenology metrics. These products broadly capture vegetation life-cycle timing at the landscape scale (USGS EROS 2018).

Relative magnitude of growing season start and end change

We followed a procedure from Garonna et al. (2014) to compare the relative magnitude of SOS and EOS change at pixels. The following equation calculates the C-Index, where ΔSOS represents change in SOS date and ΔEOS represents change in EOS date:

$$C - \text{Index} = -1 + \frac{2 * \text{abs}(\Delta\text{SOS})}{\text{abs}(\Delta\text{SOS}) + \text{abs}(\Delta\text{EOS})}. \quad (4)$$

The C-Index is bound from − 1 to 1. Negative values indicate EOS change is of greater magnitude than SOS change at a location, and positive values indicate SOS change is of greater magnitude than EOS change. We calculated the C-Index at all pixels, considering the change in SOS and EOS timing in the 2090–2099 period relative to the reference period (2001–2014).

Model validation

We first evaluated the accuracy of the binomial growing season probability model to predict whether days fell within the growing season. Binomial model predictions of at least 0.50 were interpreted as within the growing season, and predictions less than 0.50 were interpreted as not within the growing season. These predictions were compared to the original eMODIS phenology data. We evaluated the model's accuracy among training pixels in training years, validation pixels in training years, and validation pixels in validation years. These multiple lines of validation assessed whether the model was overfit to the input data and performed similarly regardless of the year and location of input data.

Next, we evaluated the accuracy of the sinusoidal growing season date model to predict growing season dates from the binomial model predictions. We compared model predictions to the eMODIS data, and evaluated root mean square error (RMSE), mean absolute error (MAE), and absolute bias of the model in predicting SOS date, EOS date, and GSL. Absolute bias was calculated as the mean of all errors (positive and negative).

Results

Binomial growing season probability model

The binomial model predicted daily growing season probability with high accuracy, and results were very similar between training and validation data. Among validation pixels in validation years, the model's accuracy was 87.05%. Therefore, in 87.05% of instances, the model correctly predicted whether a date fell within the growing season or not (with probabilities less than 0.50 considered not within the growing season, and probabilities of at least 0.50 considered within the growing season). Prediction accuracy among training pixels in training years was 87.27%, and prediction accuracy among validation pixels in training years was 87.59%. Type III ANOVA showed all variables included in the binomial model were highly significant, besides the interaction of solar radiation, vapor pressure deficit, and accumulated growing degree days (Table S1).

Sinusoidal growing season dates model

The sinusoidal model fit daily growing season probability predictions closely. Figure 3 shows the daily growing season probabilities predicted by the binomial model, and the sinusoidal model fit to daily growing season probabilities in the year 2001 for a single pixel located at 40.979 N, 115.939 W (near Elko, Nevada). In this instance, the SOS date was predicted as day 82, while eMODIS showed the SOS date was day 74, an error of 8 days. The predicted EOS date was 318, while eMODIS showed EOS date was day 321, an error of − 3 days. Predicted GSL was 236 days, and GSL from eMODIS was 247 days, an error of − 11 days. Negative errors indicate the model predicted earlier SOS/EOS dates than eMODIS, or a shorter growing season length.

Growing season dates were modeled with reasonable accuracy overall. Considering only validation years withheld from modeling, the mean MAE of modeled SOS dates across the study area was 19.46 days, mean RMSE was 22.85 days, and mean absolute bias was -5.24 days (Fig. S1). EOS dates were modeled with similar accuracy. Mean MAE was 21.80, mean RMSE was 27.04, and bias was 0.97 (Fig. S2). Errors modeling GSL were slightly higher. Mean MAE of GSL was 23.69, mean RMSE was 27.92, and bias was 6.21 (Fig. S3).

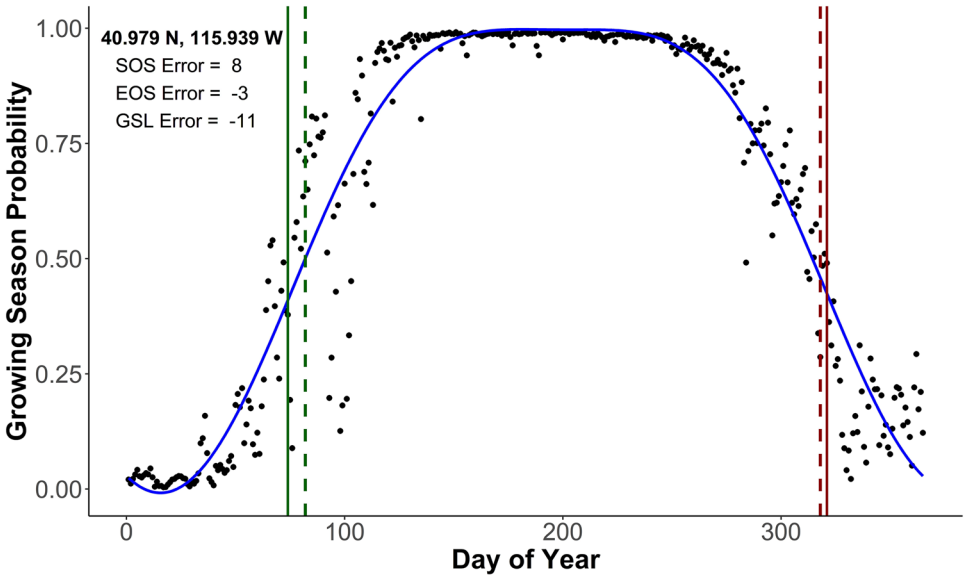

Fig. 3 Daily growing season probabilities predicted by the binomial model at a pixel near Elko, Nevada in 2001 (points). Blue line is the sinusoidal model fit to daily growing season probabilities. Dashed vertical lines indicate the SOS and EOS dates determined by the sinusoidal model, and solid vertical lines indicate the SOS and EOS dates from eMODIS at this pixel in 2001. Green lines indicate SOS, and red lines indicate EOS

Future projected growing season dates

Future growing season dates projected by the models showed significant changes relative to the historical reference period (2001–2014). SOS dates were projected to advance throughout the region, and advance more dramatically in RCP 8.5 than 4.5 (Fig. 4). In results from the ensemble model, approximately half of the region was projected to experience SOS advancement of at least 5 days by the 2030–2039 period in both RCP 4.5 and 8.5 (Fig. 4a, d). By the 2090–2099 period, start of season dates were projected to advance at least 5 days in nearly the entire region, with more intense advancement under the RCP 8.5 scenario (Fig. 4c, f). In this latest time period, mean advancement in the RCP 4.5 ensemble was 9.88 days, while mean advancement in the RCP 8.5 scenario was 16.82 days. These correspond to a rate of change through 2090–2099 of 0.12 days per year in RCP 4.5, and 0.21 days per year in RCP 8.5. SOS advancement was greatest throughout southern Idaho, eastern Washington, and eastern Oregon, with SOS projected to arrive as much as 30 days earlier by the end of the century in these areas.

EOS dates were also mainly projected to advance, and more dramatically in RCP 8.5 than 4.5 (Fig. 5). Overall, EOS advanced by greater magnitude than SOS, and by the 2090–2099 period most areas had EOS advancement of at least 10 days. Mean advancement in 2090–2099 was 12.47 days in RCP 4.5, and 24.17 days in RCP 8.5 (Fig. 5c, f). The respective rates of change were 0.16 days per year for RCP 4.5, and 0.30 days per year for RCP 8.5. However, isolated areas in the Rocky Mountains demonstrated EOS delays in all time periods and both RCPs, contrary to results elsewhere.

GSL was not projected to change as much as either SOS or EOS (Fig. 6). GSL change was modest until the 2060–2069 period, when mean GSL contraction was 2.50 days in RCP 4.5 and 5.06 days in RCP 8.5 (Fig. 6b, e). Changes through the 2090–2099 period were similar, but with more extreme contraction in southern areas in the RCP 8.5 scenario, and with mean GSL shortening by an additional 2.29 days. Mean GSL shortening in this period was 2.59 days under RCP 4.5 (a rate of 0.03 days per year), and 7.35 days under RCP 8.5 in 2090–2099 (a rate of 0.09 days per year). In all time periods and RCP scenarios, both GSL contraction and expansion were evident in some areas, with expansion in isolated areas in the Rocky Mountains.

Considering projected changes in individual ecological provinces allows for finer comparisons between regions (Fig. 7). Though isolated areas had EOS delays projected (Fig. 5), no ecological province as a whole was projected to experience a delay in EOS (Fig. 7b). The Middle Rocky Mountain Steppe and Southern Rocky Mountain Steppe had broad spreads in EOS dates due to the areas projected to experience EOS delays, but mean EOS in these provinces as a whole was still projected to advance. By the end of the century, mean EOS advancement approached 30 days in some provinces under RCP 8.5, but was closer to 10 days under RCP 4.5.

SOS changes were fairly consistent between provinces (Fig. 7a). Unlike for EOS, no areas were projected to experience later SOS. By the end of the century, SOS advancement was around 10 days for all provinces in RCP 4.5, and nearly 20 days in RCP 8.5. For both EOS and SOS change, projections for RCP 4.5 and 8.5 did not strongly differ from one another until approximately 2060.

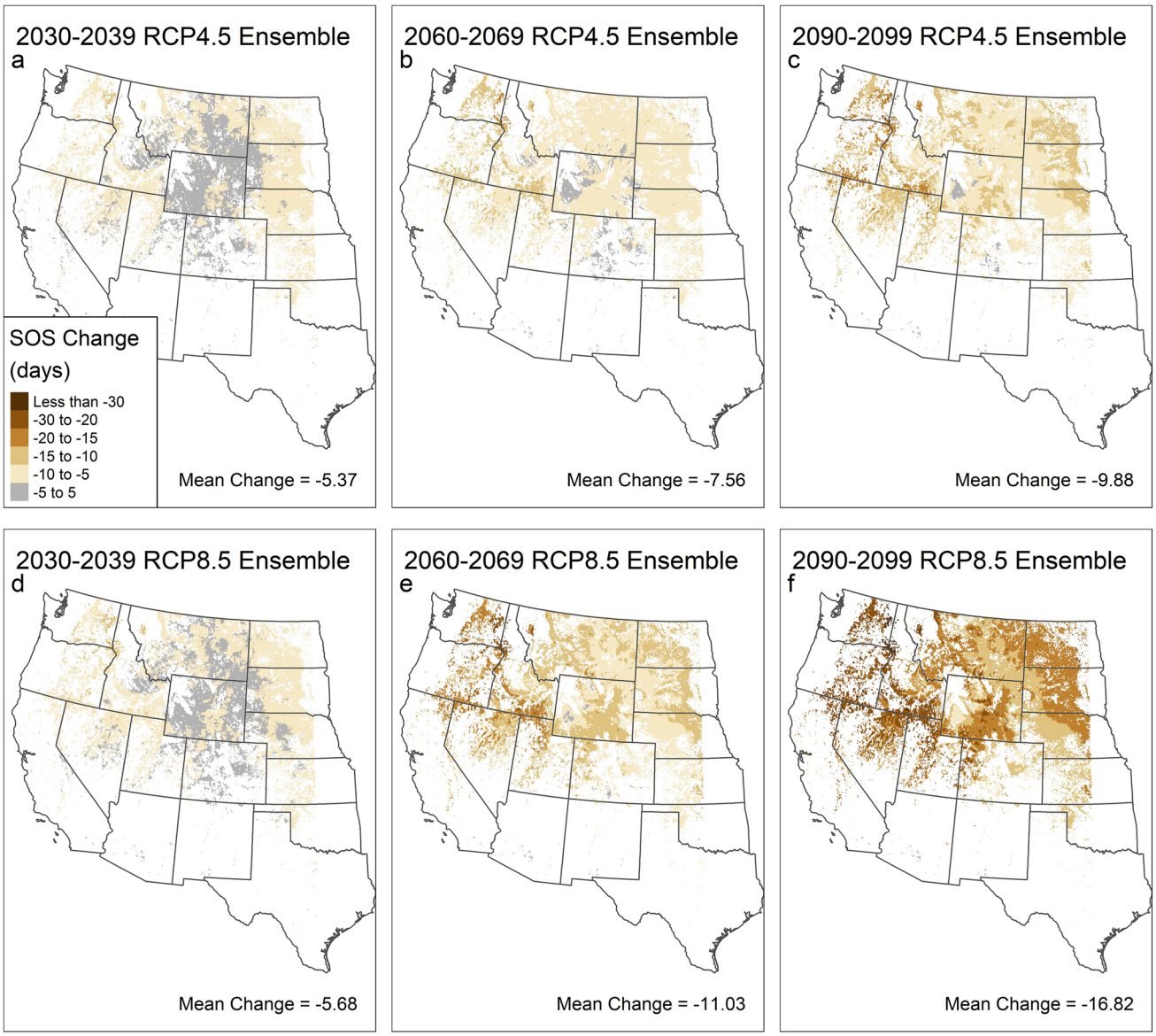

Fig. 4 Mean projected start of season date change among the ensemble of all six included GCMs, among RCP 4.5 (**a**–**c**) and RCP 8.5 (**d**–**f**) scenarios

Large GSL shifts were not projected for any ecological provinces as a whole (Fig. 7c). In all provinces, GSL was shorter in the RCP 8.5 projections than RCP 4.5. Mean GSL decreases in RCP 8.5 ranged from 5 to 10 days in all provinces, while nearly no GSL change was projected under RCP 4.5. The Middle Rocky Mountain Steppe and Southern Rocky Mountain Steppe had broad GSL change spreads, and indicated a slightly lengthened growing season by the end of the century under RCP 4.5.

Relative magnitude of growing season start and end change

In both RCP 4.5 and 8.5, the C-Index, measuring the relative magnitude of SOS and EOS change, was negative in most of the study area (Fig. 8). This indicates EOS change was of greater magnitude than SOS change in most locations. The mean C-Index throughout the study area was -0.13 in RCP 4.5 and -0.17 in RCP 8.5. However, in both RCP 4.5 and 8.5, isolated areas of the Rocky Mountains had positive C-Index values, indicating greater changes in SOS than EOS.

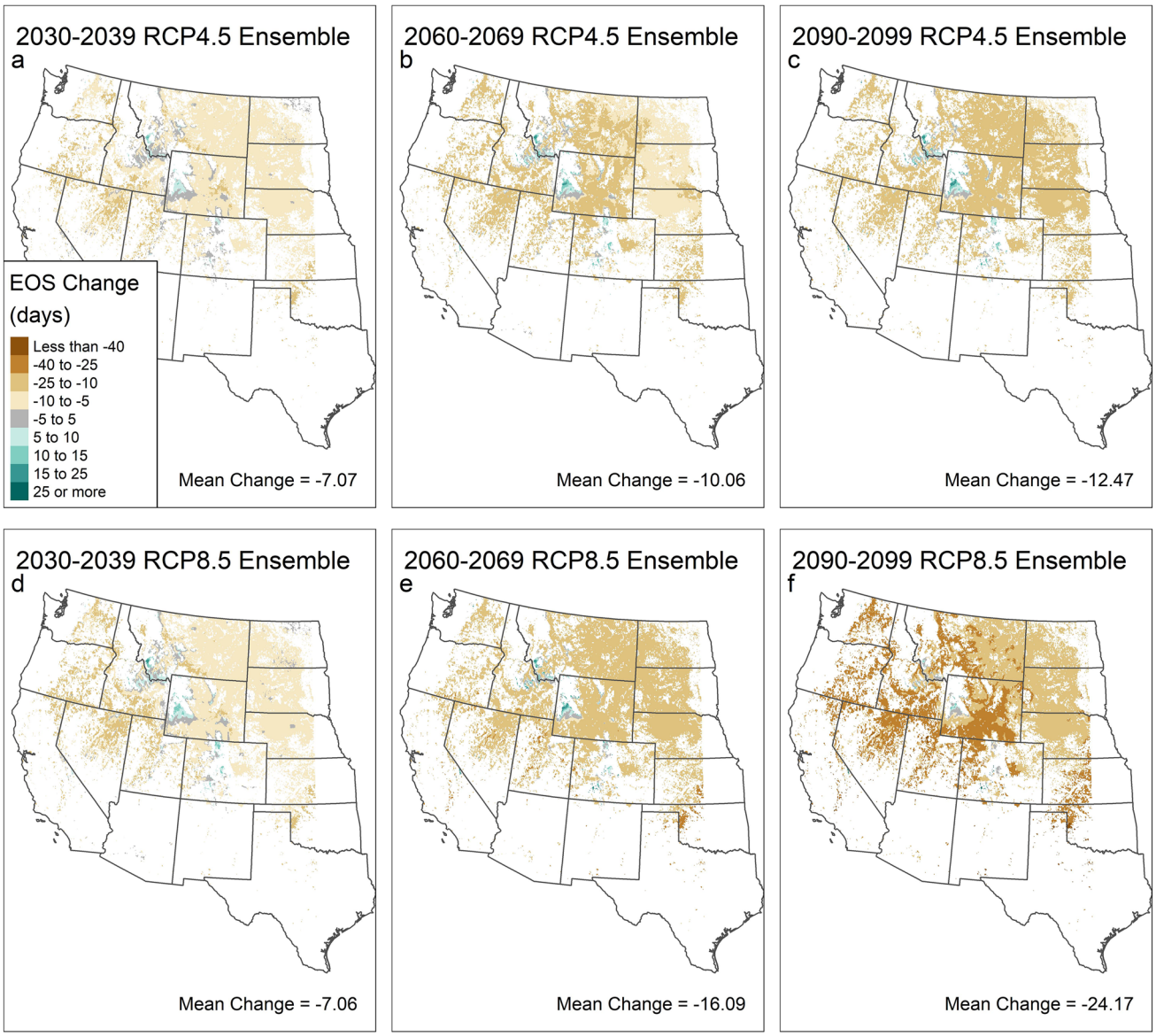

Fig. 5 Mean projected end of season date change among the ensemble of all six included GCMs, among RCP 4.5 (**a**–**c**) and RCP 8.5 (**d**–**f**) scenarios

Discussion

Projected growing season changes

We trained a model on eMODIS phenology products, which represent the timing of vegetation growing seasons at a landscape scale, to project future changes in growing season timing and length. Our results indicated both start of season and end of season timing will occur earlier in response to future climate change in the majority of our study area (Figs. 4, 5). Overall impacts to growing season length were less pronounced, but tended toward slight contraction in most areas, with some mountainous areas experiencing growing season extension (Fig. 6).

Studies of grassland growing season shifts in response to recent climate change have typically shown advancement in spring green-up (Piao et al. 2007; Zhang et al. 2013; Li et al. 2016; Ren et al. 2018b). Impacts to autumn senescence timing are more varied, but studies in grasslands have mainly found advancement (Li et al. 2016; Ren et al. 2018a, b; Ying et al. 2020).

However, comparable studies to ours projecting future phenological shifts in grasslands are rare. A study in

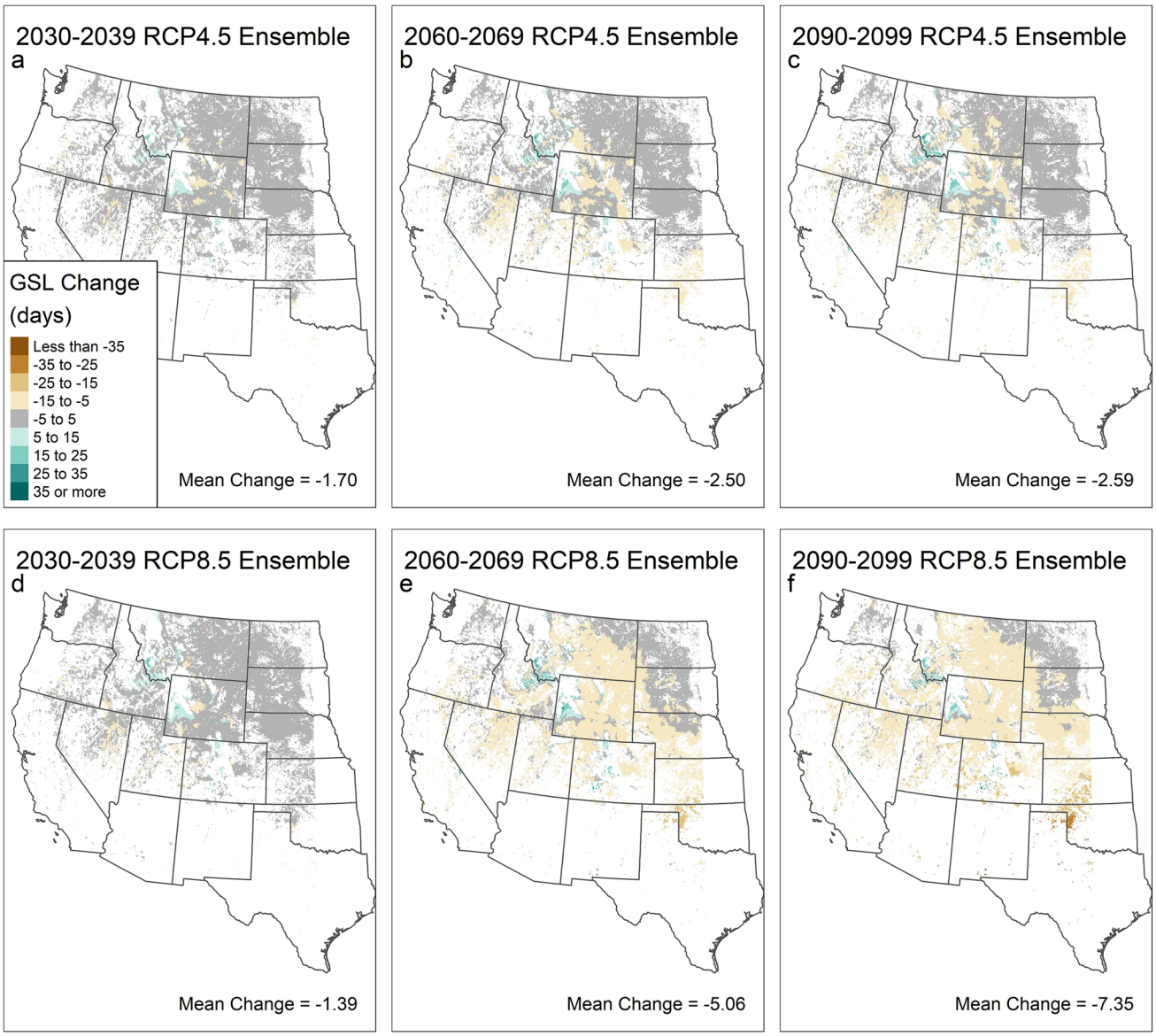

Fig. 6 Mean projected growing season length change among the ensemble of all six included GCMs, among RCP 4.5 (**a**–**c**) and RCP 8.5 (**d**–**f**) scenarios

European grasslands found similar results, with a widespread shift toward earlier start of season timing largely outweighed by a corresponding advancement in end of season timing, resulting in growing season length contraction (Chang et al. 2017). This study found increasing spring temperatures advanced spring green-up, while increased summer aridity from high temperatures and low moisture advanced autumn senescence. These effects have also been demonstrated experimentally (Zavaleta et al. 2003). A recent study found experimental warming of cheatgrass had the same results, with earlier flowering, earlier senescence, and shortened growing season (Howell et al. 2020).

However, another study of future phenology in our study area projected earlier start of season, later end of season, and longer growing season length (Hufkens et al. 2016). This study projected reductions in productivity and vegetation cover during summer drought, which were then reversed with increased activity during autumn. Our sinusoidal model did not allow for multiple growing seasons in a year, and assumed vegetation could not enter the growing season again once growing season probability began to decrease. This may account for the discrepancy between our results and those of Hufkens et al. (2016).

Some research in forests and grasslands has shown that start of season and end of season dates are positively

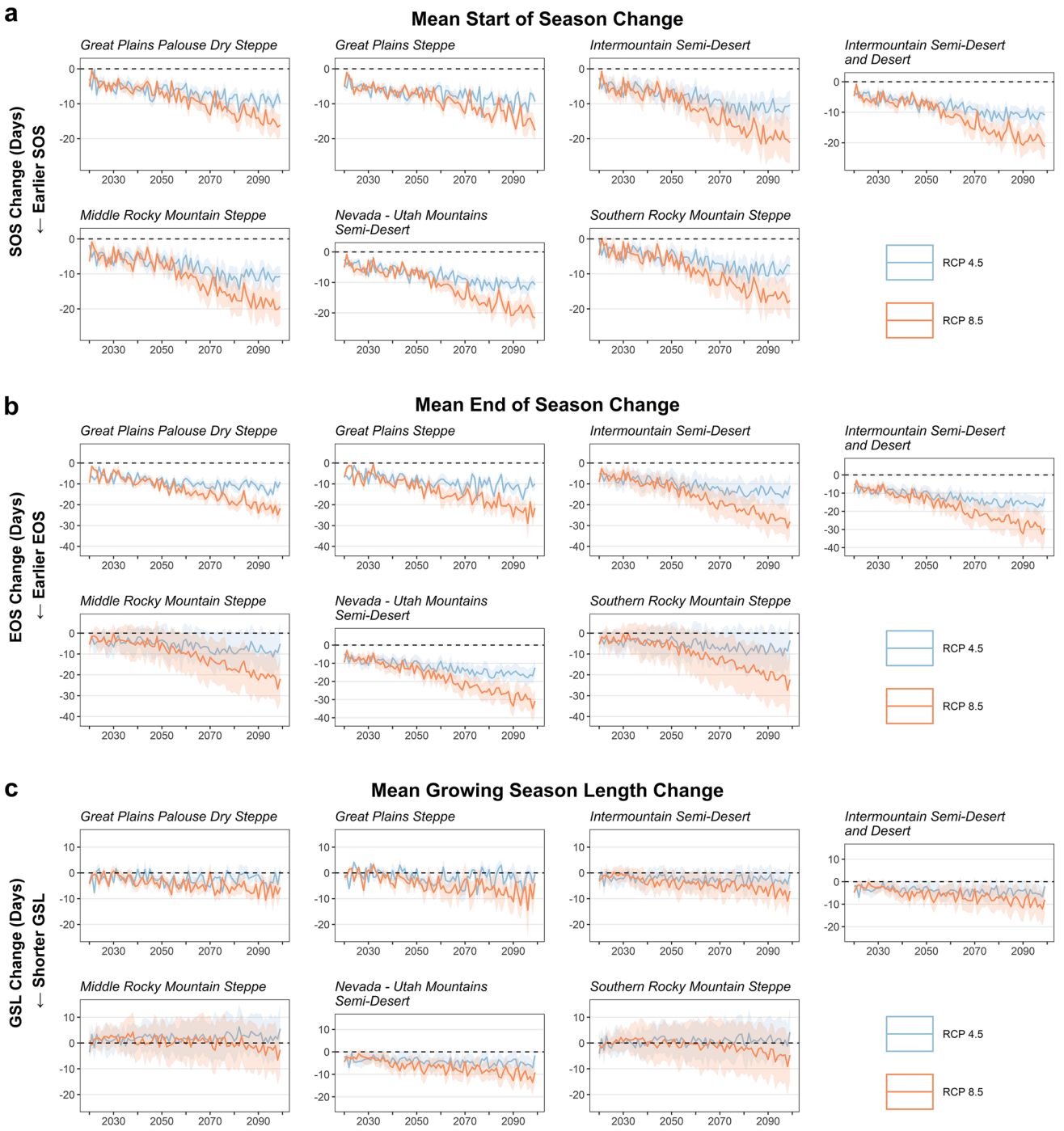

Fig. 7 Mean projected SOS (**a**), EOS (**b**), and GSL (**c**) change in ecological provinces among the ensemble of all six included GCMs, for both RCP 4.5 and RCP 8.5 scenarios. Lines represent mean results by year, and shading indicates one standard deviation from the mean

correlated, and thus likely to shift in the same direction, as we found (Fu et al. 2014; Keenan and Richardson 2015; Wu et al. 2016). Explanations for this relationship are numerous, and more research into this phenomenon is needed. Possibilities include limits of leaf longevity and programmed cell death (Keenan and Richardson 2015), or plant circadian rhythms (McWatters and Devlin 2011; Zu et al. 2018). Other hypotheses suggest that carbon-sink limitations force vegetation senescence when maximum carbohydrate reserves are reached, promoting earlier senescence following earlier green-up (Fu et al. 2014; Zani et al. 2020).

Though our model did not explicitly incorporate this effect, the constraint imposed by accumulated growing

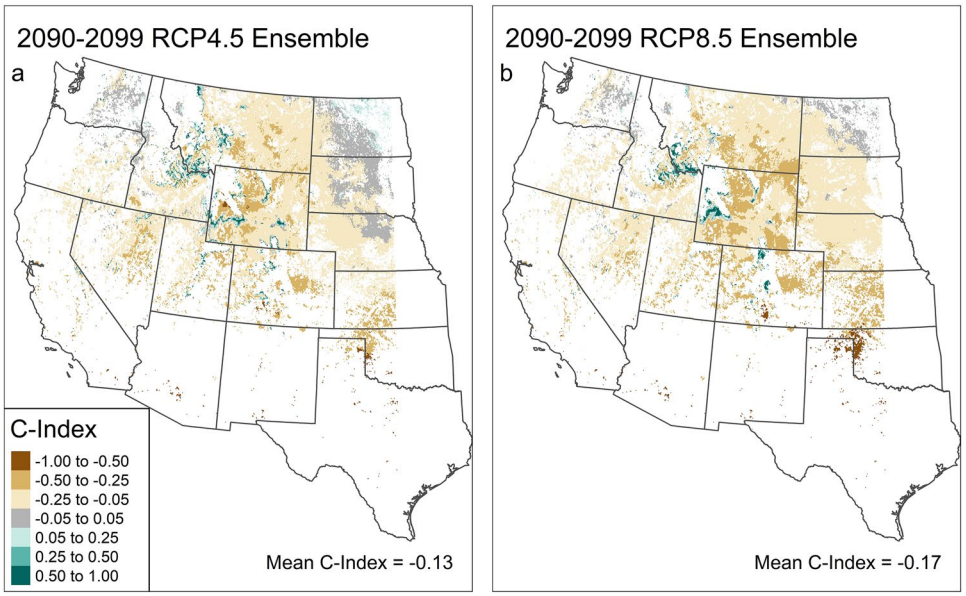

Fig. 8 Mean projected C-Index, considering mean SOS and EOS change from 2090 to 2099 relative to the reference period (2001–2014)

degree days worked similarly in our model. However, we found end of season timing was delayed while growing seasons lengthened in higher elevation grasslands in the Rocky Mountains, in contrast to other areas. This may be because these cooler, moister grasslands are temperature limited so warmer temperatures can extend their growing season, whereas moisture limitations are more significant in the drier, lower elevation grasslands through the rest of our study area (White et al. 1997).

Importance of end of season timing

Changes in end of season timing, and autumn phenology generally, have not received as much attention as start of season or spring phenology (Gallinat et al. 2015; Piao et al. 2019). Our C-Index calculation suggested end of season timing will change more than start of season timing throughout most of our study area (Fig. 8), supporting the importance of considering autumn phenology in any consideration of phenology impacts. Though end of season change may not always be of greater magnitude than start of season change, it is clearly an important aspect of phenology research that cannot be ignored. Autumn phenology impacts are generally more varied than spring phenology impacts (Walther et al. 2002; Richardson et al. 2013), and controls on autumn phenology are less clear than those on spring phenology (Ren et al. 2018a; Fu et al. 2020), so better discernment of these controls by ecosystem and region are still needed. Our results also support the finding that autumn phenology impacts are more varied than spring impacts, with both end of season advancement and delay projected in our results.

Impacts to ecosystems and ecosystem management

Livestock grazing is a dominant land use in our study area and would be impacted by phenological shifts, requiring adaptation for effective management (Rojas-Downing et al. 2017; Ren et al. 2018b). Earlier growing seasons will likely force ranchers to bring livestock to pasture earlier in the year, but contracting growing season length could reduce the amount of time livestock can graze vegetation within the growing season, potentially increasing ranchers' demands for supplemental winter feed.

Changing climate will also have direct impacts on livestock grazing which interact with phenology. For example, heat stress induced by high temperatures and humidity can reduce cattle weight gain and health, and increase water demands (Howden et al. 2008; Polsky and von Keyserlingk 2017). Indirect effects of heat on livestock health, including reduced immune response and increased vector-borne illness spread are also possible (Nardone et al. 2010). These factors may challenge grazing management and reduce ranching profitability (Neibergs et al. 2018). On the other hand, higher winter temperatures and reduced snow cover could increase access to forage, even where growing season length contracts (Chang et al. 2017). Climate change will also impact forage quantity (Polley et al. 2013) and forage quality (Dumont et al. 2015), both crucial for livestock grazing.

Phenological mismatch and disruption of species interdependencies may result if species adjust phenological timing differently in response to climate change (Rafferty et al. 2013). Though global shifts in phenological synchrony are apparent (Kharouba et al. 2018), evidence of phenological

mismatch in mutualistic relationships is rare (Bartomeus et al. 2011). Mismatch is more common in antagonistic or competitive relationships where species have not co-evolved common phenological strategies (Both et al. 2009; Renner and Zohner 2018).

Phenological plasticity affects species fitness, and the ability to adapt phenology could contribute to community compositions shifts in the future (Reed et al. 2013; Duputié et al. 2015). In the western US, for example, annual and cool-season grasses are more closely tracking climate change than perennial grasses or warm-season grasses (Munson and Long 2017). Similarly, invasive plants track climate change and adjust phenological timing more closely than native species (Wolkovich et al. 2013; Wolkovich and Cleland 2014). There could be significant implications if these phenological differences lead to plant community shifts, particularly as invasive annual cool-season grasses such as cheatgrass (*Bromus tectorum*) already pose significant management challenges in our study area (Knapp 1996). However, to what degree both phenotypic plasticity and genetic adaptation contribute to phenological tracking is unclear (Franks and Weis 2008), which may influence how significantly species phenology can adapt in the future.

Model error

Fitting start of season dates across the study area, our modeling method achieved a mean MAE of 19.46 days and mean RMSE of 22.85 days. End of season dates and growing season length were modeled with slightly higher error (respectively, MAE of 21.80 and RMSE of 27.04, and MAE of 23.69 and RMSE of 27.92. Xin et al. (2015) also modeled start of season timing in western U.S. grasslands using eMODIS phenology data, and their best models outperformed ours, with RMSE of 16.4 days. This indicates the potential to improve our model by incorporating either a modified growing degree day or accumulated growing season index term, as they used (Xin et al. 2015). However, Xin et al. did not address end of season timing, whereas we employed a unified model of growing season start and end, which may constrain model performance.

Errors in our model were comparable to or better than other available examples fit to satellite-derived phenology metrics. With a double logistic function fit to NDVI at two Inner Mongolia grasslands, Ren et al. (2018a) fit start of season timing with MAE from 14.7 to 15.2 days. End of season, though was fit with MAE from 32.1 to 48.1, significantly higher errors than our model. Incorporating ground-measured gross primary production measurements at five sites, Ren et al. (2018b) greatly reduced errors (RMSE of 12.9 days for start of season and 13.0 days for end of season). Therefore, incorporating remotely-sensed gross primary productivity data could improve our model, though such estimates at large spatial scales may be significantly less accurate than those from ground-based observation sites. Furthermore, future projections of such data may not be reliable, limiting the ability to project a model based on gross primary productivity into the future.

Limitations

We used a relatively simple model which projected growing season timing based on readily-available future climatic data, and did not consider factors beyond climate which could impact phenology. Carbon dioxide (CO_2) concentrations were not included in our model, but CO_2 concentration influences vegetative productivity in numerous ways (Polley et al. 2013), and increased concentrations may lengthen growing seasons through increased species complementarity (Reyes-Fox et al. 2014). Disturbances associated with climate change, such as wildfire, were also not included in our model, but could alter plant communities and phenology timing as well (Wang and Zhang 2020). Growing season length itself may be mediated by plant diversity, with greater diversity promoting a longer growing season (Oehri et al. 2017), but we could not include this effect.

Similarly, we did not consider phenological implications of shifts in vegetation type. Greater composition of warm-season grasses would shift growing season timing later in the year, but climate change impacts on the composition of warm-season and cool-season grasses are still unclear due to the offsetting impacts of increased CO_2 concentrations and increased temperatures (Ehleringer et al. 1997; Morgan et al. 2011). Our study area has also experienced shrubland and tree encroachment in recent years (Miller and Rose 1999; Knapp et al. 2008a, b), and continued shifts from grass to these species could impact phenology timing as well.

We could not analyze changes in net primary productivity (NPP), gross primary productivity (GPP), or other carbon flux measures in our model, which have important climate change implications (Cao and Woodward 1998). Many have found a positive relationship between NPP and growing season length (Myneni et al. 1997; Zhou et al. 2001; Bao et al. 2019), but this is not true in all circumstances, with differences in climatic regimes and drought occurrence playing a role (Wu et al. 2016; Wang et al. 2017). Importantly, net ecosystem productivity (NEP), which is most important from a global carbon perspective, may not increase even when GPP and NPP do, because increased soil carbon decomposition can offset increased GPP and NPP (Piao et al. 2007).

Our model assumed a single spring green-up and autumn senescence in each year. Measures like productivity vary throughout the growing season (Piao et al. 2007; Hufkens et al. 2016), but these variations and pulses in growth are not evident in our model since we modeled only the timing of growing season start and end. Climate change is likely to induce less frequent and more intense precipitation events (Trenberth 2011), potentially altering soil moisture dynamics and subsequent vegetation growth pulses in semi-arid systems (Huxman et al. 2004; Knapp et al. 2008a, b). These pulses in growth may be particularly important in autumn, as moisture limitations increase and isolated precipitation events may sustain or renew growth. eMODIS phenology products may be improved by accounting for false green-up determinations from NDVI increases following snowmelt (Beck et al. 2006; Wang et al. 2018). Though timing of growing season start in our model could be too early due to the effects of snowmelt on NDVI, we were most concerned with trends through time which should be less susceptible to these errors, rather than growing season dates themselves.

Conclusion

Phenology exerts significant control on many ecological systems, and the timing of phenological events is strongly influenced by climate. Vegetation phenology, including the timing of spring green-up and autumn senescence, is already shifting in response to climate change, and will continue to shift in the future. Our findings suggest climate change will promote earlier spring green-up and earlier autumn senescence timing in temperate U.S. rangelands. We found autumn advancement was of greater magnitude than spring advancement in most locations, which would consequently shorten overall growing season length in most places. While many phenology studies in forested ecosystems have shown growing seasons have lengthened as spring advances and autumn is delayed, findings in grasslands have mainly shown that both spring and autumn timing are advancing. The projected growing season changes we found would have important effects on livestock grazing, species fitness, and overall ecosystem function.

Supplementary Information The online version contains supplementary material available at https://doi.org/10.1007/s40808-022-01389-4.

Author contributions MCR, JRS, and SNZ designed the study. SNZ, MCR, and JRS generated and analyzed the data. SNZ wrote the manuscript with contributions from MCR, JRS, and BBH.

Funding This project was supported by the National Science Foundation under Grant No. 1633756.

Availability of data and material (data transparency) Data and material have not been made available.

Code availability (software application or custom code) Underlying code has not been made available.

Declarations

Conflict of interest The authors declare no conflicts or competing of interests.

Ethics approval Not applicable.

Consent to participate All authors declare to consent to participate in this study.

Consent for publication All authors declare to consent to the publication of this study.

References

Abatzoglou JT (2013) Development of gridded surface meteorological data for ecological applications and modelling. Int J Climatol 33:121–131. https://doi.org/10.1002/joc.3413

Abatzoglou JT, Brown TJ (2012) A comparison of statistical downscaling methods suited for wildfire applications. Int J Climatol 32:772–780. https://doi.org/10.1002/joc.2312

Bao G, Chen J, Chopping M et al (2019) Dynamics of net primary productivity on the Mongolian Plateau: joint regulations of phenology and drought. Int J Appl Earth Obs Geoinform 81:85–97. https://doi.org/10.1016/j.jag.2019.05.009

Bartomeus I, Ascher JS, Wagner D et al (2011) Climate-associated phenological advances in bee pollinators and bee-pollinated plants. PNAS 108:20645–20649. https://doi.org/10.1073/pnas.1115559108

Beck PSA, Atzberger C, Høgda KA et al (2006) Improved monitoring of vegetation dynamics at very high latitudes: a new method using MODIS NDVI. Remote Sens Environ 100:321–334. https://doi.org/10.1016/j.rse.2005.10.021

Both C, van Asch M, Bijlsma RG et al (2009) Climate change and unequal phenological changes across four trophic levels: constraints or adaptations? J Anim Ecol 78:73–83. https://doi.org/10.1111/j.1365-2656.2008.01458.x

Boyte SP, Wylie BK, Major DJ (2015) Mapping and monitoring cheatgrass dieoff in rangelands of the northern Great Basin, USA. Rangel Ecol Manag 68:18–28. https://doi.org/10.1016/j.rama.2014.12.005

Brown JF (2016) Conterminous United States remote sensing phenology metrics database. https://doi.org/10.5066/F7PC30G1

Cao M, Woodward FI (1998) Dynamic responses of terrestrial ecosystem carbon cycling to global climate change. Nature 393:249–252. https://doi.org/10.1038/30460

Chang J, Ciais P, Viovy N et al (2017) Future productivity and phenology changes in European grasslands for different warming levels: implications for grassland management and carbon

balance. Carbon Balance Manag 12:11. https://doi.org/10.1186/s13021-017-0079-8
Cleland E, Chuine I, Menzel A et al (2007) Shifting plant phenology in response to global change. Trends Ecol Evol 22:357–365. https://doi.org/10.1016/j.tree.2007.04.003
Delbart N, Toan TL, Kergoat L, Fedotova V (2006) Remote sensing of spring phenology in boreal regions: a free of snow-effect method using NOAA-AVHRR and SPOT-VGT data (1982–2004). Remote Sens Environ 1:52–62. https://doi.org/10.1016/j.rse.2005.11.012
Dumont B, Andueza D, Niderkorn V et al (2015) A meta-analysis of climate change effects on forage quality in grasslands: specificities of mountain and Mediterranean areas. Grass Forage Sci 70:239–254. https://doi.org/10.1111/gfs.12169
Duputié A, Rutschmann A, Ronce O, Chuine I (2015) Phenological plasticity will not help all species adapt to climate change. Glob Change Biol 21:3062–3073. https://doi.org/10.1111/gcb.12914
Ehleringer JR, Cerling TE, Helliker BR (1997) C4 photosynthesis, atmospheric CO2, and climate. Oecologia 112:285–299. https://doi.org/10.1007/s004420050311
Estrella N, Menzel A (2006) Responses of leaf colouring in four deciduous tree species to climate and weather in Germany. Clim Res 32:253–267. https://doi.org/10.3354/cr032253
Frank AB, Hofmann L (1989) Relationship among grazing management, growing degree-days, and morphological development for native grasses on the Northern Great Plains. J Range Manag. https://doi.org/10.2307/3899472
Franks SJ, Weis AE (2008) A change in climate causes rapid evolution of multiple life-history traits and their interactions in an annual plant. J Evol Biol 21:1321–1334. https://doi.org/10.1111/j.1420-9101.2008.01566.x
Fu YSH, Campioli M, Vitasse Y et al (2014) Variation in leaf flushing date influences autumnal senescence and next year's flushing date in two temperate tree species. Proc Natl Acad Sci 111:7355–7360. https://doi.org/10.1073/pnas.1321727111
Fu Y, Li X, Zhou X et al (2020) Progress in plant phenology modeling under global climate change. Sci China Earth Sci 63:1237–1247. https://doi.org/10.1007/s11430-019-9622-2
Gallant AL, Sadinski W, Brown JF et al (2018) Challenges in complementing data from ground-based sensors with satellite-derived products to measure ecological changes in relation to climate—lessons from temperate wetland-upland landscapes. Sensors 18:880. https://doi.org/10.3390/s18030880
Gallinat AS, Primack RB, Wagner DL (2015) Autumn, the neglected season in climate change research. Trends Ecol Evol 30:169–176. https://doi.org/10.1016/j.tree.2015.01.004
Garonna I, de Jong R, de Wit AJW et al (2014) Strong contribution of autumn phenology to changes in satellite-derived growing season length estimates across Europe (1982–2011). Glob Change Biol 20:3457–3470. https://doi.org/10.1111/gcb.12625
Garroutte EL, Hansen AJ, Lawrence RL (2016) Using NDVI and EVI to map spatiotemporal variation in the biomass and quality of forage for migratory elk in the Greater Yellowstone Ecosystem. Remote Sens 8:404. https://doi.org/10.3390/rs8050404
Ge Q, Wang H, Rutishauser T, Dai J (2015) Phenological response to climate change in China: a meta-analysis. Glob Change Biol 21:265–274. https://doi.org/10.1111/gcb.12648
Girondot M, Rivalan P, Wongsopawiro R et al (2006) Phenology of marine turtle nesting revealed by statistical model of the nesting season. BMC Ecol 6:11. https://doi.org/10.1186/1472-6785-6-11
Gu Y, Wylie BK, Bliss NB (2013) Mapping grassland productivity with 250-m eMODIS NDVI and SSURGO database over the Greater Platte River Basin, USA. Ecol Ind 24:31–36. https://doi.org/10.1016/j.ecolind.2012.05.024
Hanes JM, Liang L, Morisette JT (2014) Land surface phenology. In: Hanes JM (ed) Biophysical applications of satellite remote sensing. Springer Berlin Heidelberg, Berlin, Heidelberg, pp 99–125
Henebry GM, de Beurs KM (2013) Remote sensing of land surface phenology: a prospectus. In: Schwartz MD (ed) Phenology: an integrative environmental science. Springer Netherlands, Dordrecht, pp 385–411
Hogg EH, Price DT, Black TA (2000) Postulated feedbacks of deciduous forest phenology on seasonal climate patterns in the western Canadian interior. J Clim 13:4229–4243. https://doi.org/10.1175/1520-0442(2000)013%3c4229:PFODFP%3e2.0.CO;2
Howard DM, Wylie BK, Tieszen LL (2012) Crop classification modelling using remote sensing and environmental data in the Greater Platte River Basin, USA. Int J Remote Sens 33:6094–6108. https://doi.org/10.1080/01431161.2012.680617
Howden SM, Crimp SJ, Stokes CJ et al (2008) Climate change and Australian livestock systems: impacts, research and policy issues. Aust J Exp Agric 48:780–788. https://doi.org/10.1071/EA08033
Howell A, Winkler DE, Phillips ML et al (2020) Experimental warming changes phenology and shortens growing season of the dominant invasive plant *Bromus tectorum* (cheatgrass). Front Plant Sci 11:1528. https://doi.org/10.3389/fpls.2020.570001
Hufkens K, Keenan TF, Flanagan LB et al (2016) Productivity of North American grasslands is increased under future climate scenarios despite rising aridity. Nat Clim Change 6:710–714. https://doi.org/10.1038/nclimate2942
Huxman TE, Snyder KA, Tissue D et al (2004) Precipitation pulses and carbon fluxes in semiarid and arid ecosystems. Oecologia 141:254–268. https://doi.org/10.1007/s00442-004-1682-4
Jenkerson CB, Maiersperger T, Schmidt G (2010) eMODIS: a user-friendly data source
Jeong S-J, Ho C-H, Gim H-J, Brown ME (2011) Phenology shifts at start vs. end of growing season in temperate vegetation over the Northern Hemisphere for the period 1982–2008. Glob Change Biol 17:2385–2399. https://doi.org/10.1111/j.1365-2486.2011.02397.x
Jolly WM, Nemani R, Running SW (2005) A generalized, bioclimatic index to predict foliar phenology in response to climate. Glob Change Biol 11:619–632. https://doi.org/10.1111/j.1365-2486.2005.00930.x
Joyce LA, Coulson D (2020) Climate scenarios and projections: a technical document supporting the USDA Forest Service 2020 RPA Assessment. Gen Tech Rep RMRS-GTR-413 Fort Collins, CO: US Department of Agriculture, Forest Service, Rocky Mountain Research Station, p 85. https://doi.org/10.2737/RMRS-GTR-413
Julien Y, Sobrino JA (2009) Global land surface phenology trends from GIMMS database. Int J Remote Sens 30:3495–3513. https://doi.org/10.1080/01431160802562255
Keenan TF, Richardson AD (2015) The timing of autumn senescence is affected by the timing of spring phenology: implications for predictive models. Glob Change Biol 21:2634–2641. https://doi.org/10.1111/gcb.12890
Kharouba HM, Ehrlén J, Gelman A et al (2018) Global shifts in the phenological synchrony of species interactions over recent decades. PNAS 115:5211–5216. https://doi.org/10.1073/pnas.1714511115
Knapp PA (1996) Cheatgrass (*Bromus tectorum* L) dominance in the Great Basin Desert: history, persistence, and influences to human activities. Glob Environ Change 6:37–52. https://doi.org/10.1016/0959-3780(95)00112-3
Knapp AK, Beier C, Briske DD et al (2008a) Consequences of more extreme precipitation regimes for terrestrial ecosystems. Bioscience 58:811–821. https://doi.org/10.1641/B580908

Knapp AK, Briggs JM, Collins SL et al (2008b) Shrub encroachment in North American grasslands: shifts in growth form dominance rapidly alters control of ecosystem carbon inputs. Glob Change Biol 14:615–623. https://doi.org/10.1111/j.1365-2486.2007.01512.x

Leopold A, Jones SE (1947) A phenological record for Sauk and Dane counties, Wisconsin, 1935–1945. Ecol Monogr 17:81–122. https://doi.org/10.2307/1948614

Li Q, Xu L, Pan X et al (2016) Modeling phenological responses of Inner Mongolia grassland species to regional climate change. Environ Res Lett 11:015002. https://doi.org/10.1088/1748-9326/11/1/015002

Liebezeit JR, Gurney KEB, Budde M et al (2014) Phenological advancement in arctic bird species: relative importance of snow melt and ecological factors. Polar Biol 37:1309–1320. https://doi.org/10.1007/s00300-014-1522-x

Lieth H (ed) (1974) Phenology and seasonality modeling. Springer-Verlag, Berlin Heidelberg

Linderholm HW (2006) Growing season changes in the last century. Agric for Meteorol 137:1–14. https://doi.org/10.1016/j.agrformet.2006.03.006

Liu Q, Fu YH, Zeng Z et al (2016) Temperature, precipitation, and insolation effects on autumn vegetation phenology in temperate China. Glob Change Biol 22:644–655. https://doi.org/10.1111/gcb.13081

Lobell DB, Roberts MJ, Schlenker W et al (2014) Greater sensitivity to drought accompanies maize yield increase in the US Midwest. Science 344:516–519. https://doi.org/10.1126/science.1251423

McNab WH, Cleland DT, Freeouf JA et al (2007) Description of ecological subregions: sections of the conterminous United States. US Department of Agriculture Forest Service, Washington

McWatters HG, Devlin PF (2011) Timing in plants—a rhythmic arrangement. FEBS Lett 585:1474–1484. https://doi.org/10.1016/j.febslet.2011.03.051

Meier GA, Brown JF (2014) Remote sensing of land surface phenology: US Geological Survey fact sheet. https://doi.org/10.3133/fs20143052

Meier GA, Brown JF, Evelsizer RJ, Vogelmann JE (2015) Phenology and climate relationships in aspen (*Populus tremuloides* Michx.) forest and woodland communities of southwestern Colorado. Ecol Ind 48:189–197. https://doi.org/10.1016/j.ecolind.2014.05.033

Menzel A (2002) Phenology: Its importance to the global change community. Clim Change 54:379–385. https://doi.org/10.1023/A:1016125215496

Miller RF, Rose JA (1999) Fire history and western juniper encroachment in sagebrush steppe. J Range Manag 52:550–559. https://doi.org/10.2307/4003623

Monteith KL, Bleich VC, Stephenson TR et al (2011) Timing of seasonal migration in mule deer: effects of climate, plant phenology, and life-history characteristics. Ecosphere 2:art47. https://doi.org/10.1890/ES10-00096.1

Morgan JA, LeCain DR, Pendall E et al (2011) C4 grasses prosper as carbon dioxide eliminates desiccation in warmed semi-arid grassland. Nature 476:202–205. https://doi.org/10.1038/nature10274

Morisette JT, Duffy KA, Weltzin JF et al (2021) PS3: The pheno-synthesis software suite for integration and analysis of multi-scale, multi-platform phenological data. Eco Inform 65:101400. https://doi.org/10.1016/j.ecoinf.2021.101400

Munson SM, Long AL (2017) Climate drives shifts in grass reproductive phenology across the western USA. New Phytol 213:1945–1955. https://doi.org/10.1111/nph.14327

Myneni RB, Keeling CD, Tucker CJ et al (1997) Increased plant growth in the northern high latitudes from 1981 to 1991. Nature 386:698–702. https://doi.org/10.1038/386698a0

Nardone A, Ronchi B, Lacetera N et al (2010) Effects of climate changes on animal production and sustainability of livestock systems. Livest Sci 130:57–69. https://doi.org/10.1016/j.livsci.2010.02.011

Neibergs JS, Hudson TD, Kruger CE, Hamel-Rieken K (2018) Estimating climate change effects on grazing management and beef cattle production in the Pacific Northwest. Clim Change 146:5–17. https://doi.org/10.1007/s10584-017-2014-0

Oehri J, Schmid B, Schaepman-Strub G, Niklaus PA (2017) Biodiversity promotes primary productivity and growing season lengthening at the landscape scale. PNAS 114:10160–10165. https://doi.org/10.1073/pnas.1703928114

Parmesan C, Yohe G (2003) A globally coherent fingerprint of climate change impacts across natural systems. Nature 421:37–42. https://doi.org/10.1038/nature01286

Piao S, Friedlingstein P, Ciais P et al (2007) Growing season extension and its impact on terrestrial carbon cycle in the Northern Hemisphere over the past 2 decades. Global Biogeochem Cycles. https://doi.org/10.1029/2006GB002888

Piao S, Cui M, Chen A et al (2011) Altitude and temperature dependence of change in the spring vegetation green-up date from 1982 to 2006 in the Qinghai-Xizang Plateau. Agric for Meteorol 151:1599–1608. https://doi.org/10.1016/j.agrformet.2011.06.016

Piao S, Liu Q, Chen A et al (2019) Plant phenology and global climate change: current progresses and challenges. Glob Change Biol 25:1922–1940. https://doi.org/10.1111/gcb.14619

Polley HW, Briske DD, Morgan JA et al (2013) Climate change and North American rangelands: trends, projections, and implications. Rangel Ecol Manag 66:493–511. https://doi.org/10.2111/REM-D-12-00068.1

Polsky L, von Keyserlingk MAG (2017) Invited review: Effects of heat stress on dairy cattle welfare. J Dairy Sci 100:8645–8657. https://doi.org/10.3168/jds.2017-12651

Preister L, Kobiela B, Dixon C, DeKeyser ES (2019) A model to identify smooth brome elongation using correlation of mean stage count and accumulated growing degree days. NAAR 39:364–371. https://doi.org/10.3375/043.039.0308

R Core Team (2018) R: a language and environment for statistical computing. R Foundation for Statistical Computing, Vienna

Rafferty NE, CaraDonna PJ, Burkle LA et al (2013) Phenological overlap of interacting species in a changing climate: an assessment of available approaches. Ecol Evol 3:3183–3193. https://doi.org/10.1002/ece3.668

Reed BC (2006) Trend analysis of time-series phenology of North America derived from satellite data. Gisci Remote Sens 43:24–38. https://doi.org/10.2747/1548-1603.43.1.24

Reed BC, Brown JF, VanderZee D et al (1994) Measuring phenological variability from satellite imagery. J Veg Sci 5:703–714. https://doi.org/10.2307/3235884

Reed TE, Jenouvrier S, Visser ME (2013) Phenological mismatch strongly affects individual fitness but not population demography in a woodland passerine. J Anim Ecol 82:131–144. https://doi.org/10.1111/j.1365-2656.2012.02020.x

Reeves MC, Mitchell JE (2011) Extent of coterminous US rangelands: quantifying implications of differing agency perspectives. Rangel Ecol Manag 64:585–597. https://doi.org/10.2111/REM-D-11-00035.1

Ren S, Chen X, Lang W, Schwartz MD (2018a) Climatic controls of the spatial patterns of vegetation phenology in midlatitude grasslands of the Northern Hemisphere. J Geophys Res Biogeosci 123:2323–2336. https://doi.org/10.1029/2018JG004616

Ren S, Yi S, Peichl M, Wang X (2018b) Diverse responses of vegetation phenology to climate change in different grasslands in Inner

Mongolia during 2000–2016. Remote Sens 10:17. https://doi.org/10.3390/rs10010017
Renner SS, Zohner CM (2018) Climate change and phenological mismatch in trophic interactions among plants, insects, and vertebrates. Annu Rev Ecol Evol Syst 49:165–182. https://doi.org/10.1146/annurev-ecolsys-110617-062535
Reyes-Fox M, Steltzer H, Trlica MJ et al (2014) Elevated CO2 further lengthens growing season under warming conditions. Nature 510:259–262. https://doi.org/10.1038/nature13207
Richardson AD, Keenan TF, Migliavacca M et al (2013) Climate change, phenology, and phenological control of vegetation feedbacks to the climate system. Agric for Meteorol 169:156–173. https://doi.org/10.1016/j.agrformet.2012.09.012
Rojas-Downing MM, Nejadhashemi AP, Harrigan T, Woznicki SA (2017) Climate change and livestock: impacts, adaptation, and mitigation. Clim Risk Manag 16:145–163. https://doi.org/10.1016/j.crm.2017.02.001
Romano G, Schaumberger A, Piepho HP et al (2014) Optimal base temperature for computing growing degree-day sums to predict forage quality of mountain permanent meadow in South Tyrol. EGF at 50: The future of European grasslands Proceedings of the 25th General Meeting of the European Grassland Federation, Aberystwyth, Wales, 7–11 September 2014, pp 655–657
Sapiano MRP, Brown CW, Schollaert Uz S, Vargas M (2012) Establishing a global climatology of marine phytoplankton phenological characteristics: phytoplankton phenology characteristics. J Geophys Res Oceans. https://doi.org/10.1029/2012JC007958
Schwartz MD, Ahas R, Aasa A (2006) Onset of spring starting earlier across the Northern Hemisphere. Glob Change Biol 12:343–351. https://doi.org/10.1111/j.1365-2486.2005.01097.x
Stöckli R, Vidale PL (2004) European plant phenology and climate as seen in a 20-year AVHRR land-surface parameter dataset. Int J Remote Sens 25:3303–3330. https://doi.org/10.1080/01431160310001618149
Taylor KE, Stouffer RJ, Meehl GA (2012) An overview of CMIP5 and the experiment design. Bull Am Meteor Soc 93:485–498. https://doi.org/10.1175/BAMS-D-11-00094.1
Trenberth KE (2011) Changes in precipitation with climate change. Clim Res 47:123–138. https://doi.org/10.3354/cr00953
USGS EROS (2018) eMODIS phenology. https://doi.org/10.5066/F7MW2FBS
Walther G-R, Post E, Convey P et al (2002) Ecological responses to recent climate change. Nature 416:389–395. https://doi.org/10.1038/416389a
Wang J, Zhang X (2020) Investigation of wildfire impacts on land surface phenology from MODIS time series in the western US forests. ISPRS J Photogramm Remote Sens 159:281–295. https://doi.org/10.1016/j.isprsjprs.2019.11.027
Wang S, Zhang B, Yang Q et al (2017) Responses of net primary productivity to phenological dynamics in the Tibetan Plateau, China. Agric for Meteorol 232:235–246. https://doi.org/10.1016/j.agrformet.2016.08.020
Wang C, Chen J, Tang Y et al (2018) A novel method for removing snow melting-induced fluctuation in GIMMS NDVI3g data for vegetation phenology monitoring: a AASE study in deciduous forests of North America. IEEE J Sel Top Appl Earth Obs Remote Sens 11:800–807. https://doi.org/10.1109/JSTARS.2017.2778076
Way DA, Montgomery RA (2015) Photoperiod constraints on tree phenology, performance and migration in a warming world. Plant, Cell Environ 38:1725–1736. https://doi.org/10.1111/pce.12431
White MA, Thornton PE, Running SW (1997) A continental phenology model for monitoring vegetation responses to interannual climatic variability. Global Biogeochem Cycles 11:217–234. https://doi.org/10.1029/97GB00330
Wolkovich EM, Cleland EE (2014) Phenological niches and the future of invaded ecosystems with climate change. AoB Plants. https://doi.org/10.1093/aobpla/plu013
Wolkovich EM, Davies TJ, Schaefer H et al (2013) Temperature-dependent shifts in phenology contribute to the success of exotic species with climate change. Am J Bot 100:1407–1421. https://doi.org/10.3732/ajb.1200478
Wu X, Liu H (2013) Consistent shifts in spring vegetation green-up date across temperate biomes in China, 1982–2006. Glob Change Biol 19:870–880. https://doi.org/10.1111/gcb.12086
Wu C, Hou X, Peng D et al (2016) Land surface phenology of China's temperate ecosystems over 1999–2013: Spatial–temporal patterns, interaction effects, covariation with climate and implications for productivity. Agric for Meteorol 216:177–187. https://doi.org/10.1016/j.agrformet.2015.10.015
Xin Q, Broich M, Zhu P, Gong P (2015) Modeling grassland spring onset across the Western United States using climate variables and MODIS-derived phenology metrics. Remote Sens Environ 161:63–77. https://doi.org/10.1016/j.rse.2015.02.003
Ying H, Zhang H, Zhao J et al (2020) Effects of spring and summer extreme climate events on the autumn phenology of different vegetation types of Inner Mongolia, China, from 1982 to 2015. Ecol Ind 111:105974. https://doi.org/10.1016/j.ecolind.2019.105974
Yu H, Luedeling E, Xu J (2010) Winter and spring warming result in delayed spring phenology on the Tibetan Plateau. PNAS 107:22151–22156. https://doi.org/10.1073/pnas.1012490107
Zani D, Crowther TW, Mo L et al (2020) Increased growing-season productivity drives earlier autumn leaf senescence in temperate trees. Science 370:1066–1071. https://doi.org/10.1126/science.abd8911
Zavaleta ES, Thomas BD, Chiariello NR et al (2003) Plants reverse warming effect on ecosystem water balance. Proc Natl Acad Sci 100:9892–9893. https://doi.org/10.1073/pnas.1732012100
Zhang G, Zhang Y, Dong J, Xiao X (2013) Green-up dates in the Tibetan Plateau have continuously advanced from 1982 to 2011. Proc Natl Acad Sci 110:4309–4314. https://doi.org/10.1073/pnas.1210423110
Zhao M, Peng C, Xiang W et al (2013) Plant phenological modeling and its application in global climate change research: overview and future challenges. Environ Rev 21:1–14. https://doi.org/10.1139/er-2012-0036
Zhou L, Tucker CJ, Kaufmann RK et al (2001) Variations in northern vegetation activity inferred from satellite data of vegetation index during 1981–1999. J Geophys Res Atmos 106:20069–20083. https://doi.org/10.1029/2000JD000115
Zhou Q, Rover J, Brown J et al (2019) Monitoring landscape dynamics in central US grasslands with harmonized Landsat-8 and Sentinel-2 time series data. Remote Sens 11:328. https://doi.org/10.3390/rs11030328
Zu J, Zhang Y, Huang K et al (2018) Biological and climate factors co-regulated spatial-temporal dynamics of vegetation autumn phenology on the Tibetan Plateau. Int J Appl Earth Obs Geoinform 69:198–205. https://doi.org/10.1016/j.jag.2018.03.006